18th Australasian Fluid Mechanics Conference
Launceston, Australia
3-7 December 2012

Effect of Fuel Injection Pressure on Size and Structure of In-Cylinder Soot Particles Sampled from an Automotive-Size Optical Diesel Engine

R. Zhang and S. Kook

School of Mechanical and Manufacturing Engineering
The University of New South Wales, Sydney, NSW 2052, Australia

Abstract

The negative impacts of particulate matter emissions on human health and the environment are serious concern in developing next-generation diesel engines. Measurements of exhaust soot level and particle size distribution have been widely used to investigate this issue. In-cylinder soot volume fraction measurement using an optical engine and laser-based diagnostics has been another approach to understand diesel soot formation details. None of these measurements however provide important details of size, shape and structure of soot particles that are in the formation stage inside the engine cylinder. To bridge this gap, we performed a direct sampling of soot particles from reacting diesel jet using thermophoretic principle. The transmission electron microscope images were further analysed to obtain the number, projection area and radius of gyration of soot particles. The fuel injection pressure was selected as a parameter of interest to test this newly developed sampling technique. The in-cylinder soot particle images showed that both the amount and size of soot particles decrease with increasing injection pressure, consistent with the findings from optical/laser-based soot data in the previous studies. This result suggests that a well-known trend of decreasing exhaust soot with increasing injection pressure is a result of decreased in-cylinder soot formation.

Introduction

Diesel engines are widely used in both stationary and mobile applications, especially where high torque is needed. It is considered to be one of the most efficient and reliable power trains among existing technologies. However, the particulate matter (PM) emitted from diesel engines has a negative impact on human health and the environment. Therefore, over the past two decades, emissions regulations for diesel engines have required a reduction of diesel PM emissions by a factor of 30. Consequently, diesel PM has become and will be the major concern in developing next-generation diesel engines.

Carbon soot particles are the major components of diesel PM, which also provides the base for other toxic substances to condense on. As a result, soot particles have become of high interests in reducing the total diesel PM emissions. Various experimental methodologies have been attempted to measure diesel soot particles. The mobility sizer is the most popular tool to characterise the number and size distribution (*i.e.* mobility diameter) of soot particles in the exhaust. However, this technique has been criticised for introducing potential errors due to its inability to differentiate complex particle shapes [2]. Its application is also limited to the exhaust soot particles only. Laser-based diagnostics for optical thickness (*KL* value) or soot volume fraction of reacting diesel jet is another approach to clarify in-cylinder soot process [6-8]. However, the optical measurements cannot provide detailed information about the size, shape and structure of in-cylinder diesel soot particles.

A thermophoretic sampling and subsequent transmission electron microscope (TEM) analysis has been widely used in open flame burners [4,5,11] for morphological analysis of soot particles. This sampling technique has been applied to the diesel exhaust and unveiled size distribution and structural details of soot particles [9,10,12]. However, it is still a question whether the soot particles sampled from the exhaust would be the same as soot produced inside the cylinder. Measurements of soot at the exhaust cannot tell much about how the soot formation occurred within the reacting diesel jet. That is because there are long and complex pathways until the soot particles formed within the reacting jet reach the exhaust pipe, such as in-flame soot oxidation, in-cylinder-flow-driven late-cycle soot burn-out, a potential dilution with oil, and deposition on the surface of the combustion chamber and exhaust valves and pipes.

To address this issue, we recently performed a direct soot sampling from the reacting jet in a constant-volume combustion chamber simulating practical diesel-engine-like environments [1,6,7]. Interesting findings for in-flame soot formation details that could not be obtained from other approaches were presented. These include size and fractal dimension of soot particles, and a correspondence between the soot volume fraction and particle shapes. In this study, we further expand our knowledge on the in-cylinder soot particles by applying a similar thermophoretic soot sampling technique in an actual diesel engine.

TEM imaging and subsequent image analysis yield the number and size of soot particles. The same sampling and image analysis was repeated for various pressure drops across the injector nozzle (*i.e.* injection pressure). The injection pressure was selected as a parameter of interest because there is a well-known trend of decreasing soot levels with increasing injection pressure and therefore can serve as a good test case for the newly developed soot sampling technique.

Experiments

A single-cylinder direct-injection diesel engine was used to perform thermophoretic soot sampling directly from the diesel flame. The engine was operated using a conventional ultra-low sulfur diesel with cetane number of 46. The fuel was delivered by a Bosch common-rail system. Detailed engine specifications are listed in table 1.

A schematic of the experimental setup is illustrated in figure 1. The engine is optically accessible for various imaging diagnostics and laser-based measurements via quartz windows in the cylinder liner. For this study, one of these windows was replaced with a metal dummy window to adopt an in-cylinder soot sampling probe. An in-house designed soot sampling probe was fixed on this side dummy window where a 3-mm-diameter TEM grid made of carbon-coated copper layers with 400 meshes was held. To allow the soot sampling probe to be exposed to the reacting diesel jet, some section of the piston-bowl rim was removed

Engine Specifications	
Displacement volume	498 cc
Bore	83 mm
Stroke	92 mm
Compression ratio	15.21
Swirl ratio	1.4
Fuel Injection System	
Type	Bosch common-rail
Number of holes	1
Nozzle type	Hydro-grounded,K1.5/86
Nozzle diameter	134 µm
Hydraulic fuelling rate	400 cc / 30 s @10 MPa
Included angle	150º

Table 1. Engine Specifications

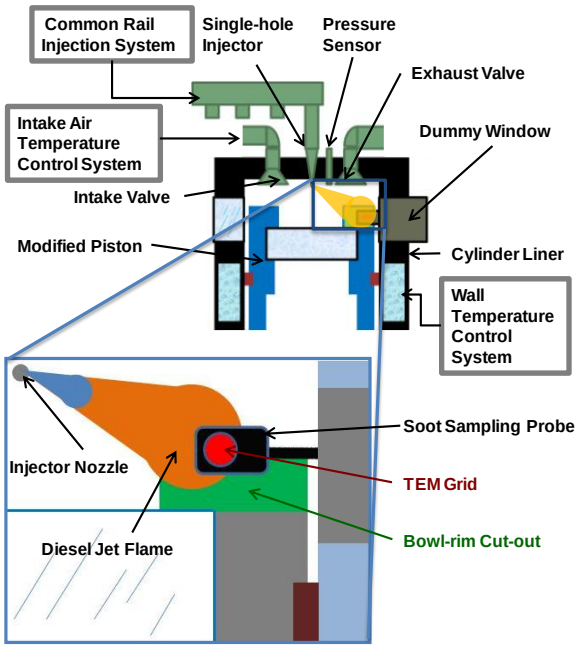

Figure 1. Cross-sectional view of the diesel engine used in this study and in-flame soot sampling system.

shown as a bowl-rim cut-out region in figure 1. The position of the sampling probe was constrained by the fast-moving engine parts including the piston and intake/exhaust valves and therefore was fixed throughout the experiments. A seven-hole conventional injector was also modified so that only one hole remained open to create a diesel jet flame directed toward the sampling probe. Since the sampling probe and the grid were an order of magnitude cooler than the sooting flame, the soot particles would be deposited on the surface of the TEM grid and a sudden quenching of soot formation and oxidation processes would occur similar to refs. [1,6,7]. Considering the position of the TEM grid and diesel flame development at a selected engine condition, it was anticipated that the sampled soot particles would be dominated by mature soot particles and partially oxidised soot particles with limited chance of having soot pre-cursors deposited on the grid 0.

Engine operating conditions are listed in table 2. The sampling experiments were conducted at a fixed engine speed of 1200 revolutions per minute (rpm) controlled by an electric motor. The injection pressure was varied from 70 to 160 MPa while all other conditions were held constant. The injection timing was fixed at 7.7 crank angle degrees before top dead centre (℃A bTDC). It

Engine speed	1200 rpm
Wall (coolant) temperature	90℃
Intake air temperature	28℃
Injection timing	7.7 ºCA bTDC
Injection pressure	70 ~ 160 MPa
Injected fuel mass per cycle	9 mg
Number of sampling cycles	5

Table 2. Engine Operating Conditions

should be noted that soot loading on TEM grid could be varied with injected fuel mass and the number of sampling cycles. In order to collect sufficient number of soot particles for statistical analysis, more injected mass and higher number of sampling cycles was preferred. However, the grid can be over-populated with a potential issue of artificial particle agglomeration. From a series of preliminary tests, these were optimised for the injected fuel mass of 9 mg per cycle and 5 sampling cycles. This means once the sampling probe was positioned inside the engine cylinder, the engine was motored at a fixed speed of 1200 rpm until 9-mg of diesel was injected at each engine cycle for 5 times while the soot particles were sampled during these 5 combustion events. The combustion conditions were monitored by measuring in-cylinder pressure using a pressure transducer (Kistler 6056A) with acquisition at every 0.072 ℃A. After 5 firing cycles, the injection was ceased and the engine was set back to the motored mode before the engine was fully stopped for collecting the TEM grid. During the engine operation, the cylinder wall temperature was fixed at 90 ℃ using a water temperature controller and circulator.

A transmission electron microscope (JEOL 1400) with a point resolution of 0.38 nm and an accelerating voltage of 120 kV was used to analyse sampled soot particles. A CCD camera with a resolution of 11 mega pixels was used to digitise magnified soot particle images. For each TEM grid, seven different grid positions were imaged considering the variations in sampled soot particles depending on the grid position. The TEM magnification was set at 50,000× to obtain a good balance between the number of particles per image and image quality for post-processing. These TEM images were then analysed using a Matlab-based image processing software for soot particle boundary detection, similar to refs. [1,6,7]. From this analysis, we obtained the projected area of soot samples, the number of particles, and particle radius of gyration.

Results and Discussions

The 5-cycle-averaged in-cylinder pressure traces and the corresponding apparent heat release rates (aHRR) for all fuel injection pressures tested in this study are shown in figure 2. These pressure traces were recorded for the same engine cycles of the soot sampling. Well-known trends are found from these traces such as decreasing ignition delay and increasing peak in-cylinder pressure with increasing injection pressure. The peak aHRR appears to be similar for the injection pressures higher than 100 MPa, which is higher than that of 70 MPa condition. Since the injected fuel mass was fixed, the observed trends were results of increased fuel-air mixing prior to the ignition (*i.e.* enhanced pre-combustion mixing) due to enhanced air entrainment. This increase in premixed combustion causes less soot formation with a chance of higher nitrogen oxide (NO_x) formation, which is known as the soot-NO_x trade-off.

An expected trend of decreasing soot with increasing injection pressure [3] is well reflected in selected TEM images shown in figure 3. The images demonstrate marked changes in the shape and structure of the diesel soot particles depending on the

injection pressure. The irregularity in shapes and fractal-like structures are not much different to those sampled in a constant volume chamber [1,5] or exhaust pipes [7-9]. However, soot particles sampled at lower injection pressure are larger than those for higher injection pressures and exhibit mature soot structures with distinct chain-like or grape-like shapes. Gigantic soot particles that are larger than the size of the scale bar (200 nm) are easily seen in the image for 70 MPa condition (figure 3a). From visual inspections, the number of particles appears to increase and then decrease with increasing injection pressure.

To specify these visual inspections, the number of soot particles and soot projection area are plotted in figure 4. As mentioned previously, multiple areas in the TEM grid were imaged. The image processing was repeated for all TEM images and the results are shown as grey circles in figure 4. Those corresponding to the selected TEM images shown in figure 3 are marked as red circles.

The first noticeable trend from figure 4 is image-to-image fluctuations. These spatial variations could be due to different exposure of the TEM grid to the sooting flame or random deposition of soot particles depending on the location on the TEM grid. While these variations are unavoidable and somewhat large for some cases, an overall trend is consistent with the observations from the images in figure 3. In other words, the number of soot particles increases with increasing injection pressure up to 100~130 MPa and then decreases as the injection pressure further increases to 160 MPa. This trend was explained by the complexity of soot formation that is varied with the injection pressure. More specifically, the soot nucleation, the particle surface growth and agglomeration would all be inhibited by high injection pressure due to enhanced fuel-air mixing as well as a limited particle residence time [8]. For instance, the number of particles for 160-MPa case is lower than that for 70-MPa case although less agglomeration is anticipated. This suggests the reduction of soot nucleation (or inception). For 100-MPa injection pressure, the soot nucleation should not be as high as at 70 MPa condition leading to lower number of particles. However, more dominant effect of limited residence time would suppress those particles to agglomerate and grow into larger sizes, resulting in higher number of particles. In contrast to the number of particles, the soot projection area (*i.e.* total amount of soot

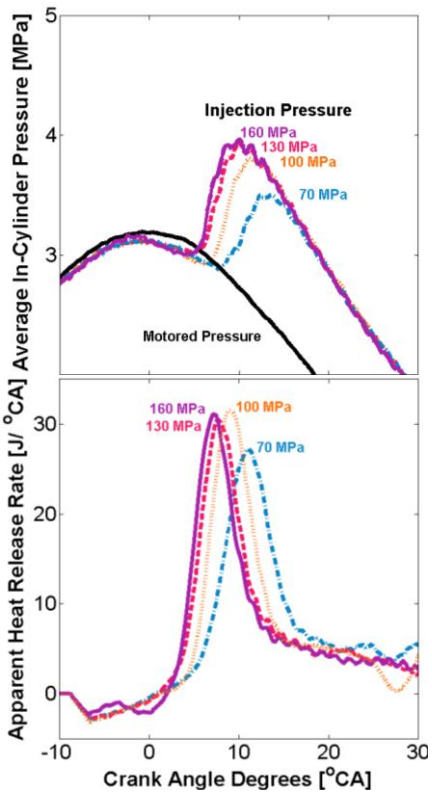

Figure 2. Average in-cylinder pressure and apparent heat release rate traces versus crank angle degree after the top dead centre (°CA aTDC) for various pressure drops across the nozzle (*i.e.* injection pressures).

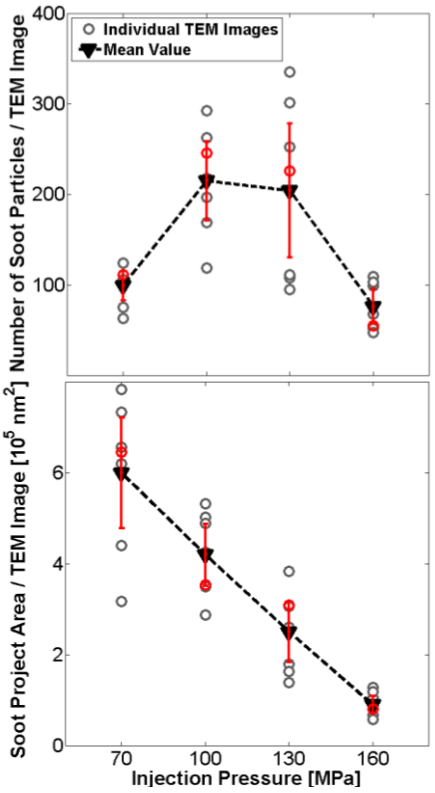

Figure 4. Number of soot particles (top) and projected soot area (bottom) per each TEM image for various injection pressures. Error bars were estimated at 95% confidence for normal distribution.

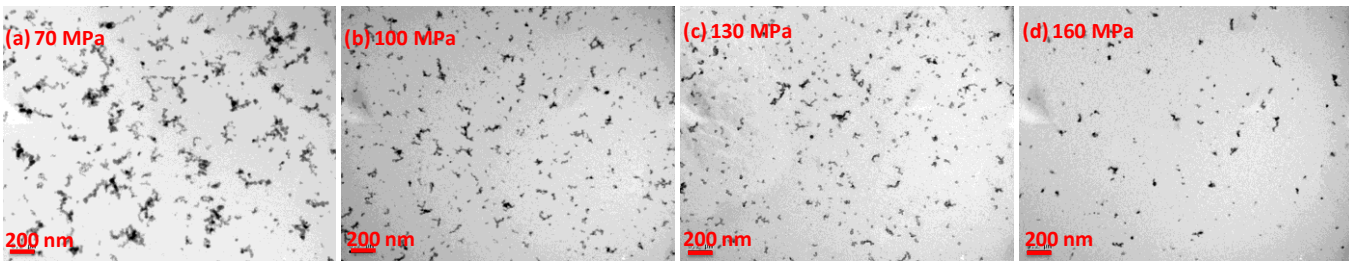

Figure 3. Transmission electron microscope images of the sampled soot particles for various injection pressures. Shown at the bottom-left corner of each image is a 200-nm scale bar.

particles) shows a linear decrease with increasing injection pressure. This is consistent with an expected trend of an overall reduction in soot formation with increasing injection pressure.

Another interesting observation from the TEM images in figure 3 was a smaller particle size at higher injection pressure. This was quantified by measuring the radius of gyration of soot particles. From the TEM images, a total number of 4163 soot particles were processed to obtain a probability density function of radius of gyration as shown in figure 5. For each injection pressure, the mean radius of gyration and an uncertainty range are also noted. Radius of gyration does decrease with increasing injection pressure, suggesting suppressed particle growth and agglomeration. A likelihood of observing gigantic soot particles decreases drastically as the injection pressure exceeds 100 MPa. One noticeable finding from figure 5 is that the radius of gyration is nearly the same for 130 and 160 MPa cases despite less number of particles as well as lower projection area (from figure 4) for 160-MPa data. This suggests very limited nucleation of soot particles at this highest injection pressure of the given common-rail system.

Conclusions

Soot particles were sampled directly from reacting diesel jet in an automotive-size diesel engine using an in-flame soot sampling probe and transmission electron microscope grid. The TEM images were post-processed to obtain the number of soot particles, projection area, and radius of gyration for various injection pressures. The major conclusions from this study can be drawn as follows:

1. A direct soot sampling from diesel flame in an engine is successfully performed. The obtained soot particles exhibit similar shapes and structures of those sampled from diesel exhaust streams and constant-volume combustion chamber at a similar condition.
2. A well-known diesel soot reduction with high injection pressure is reproduced in soot particle data. The decreased projection area and radius of gyration of soot particles suggest that the low exhaust soot level at high injection pressure condition is a result of decreased in-cylinder soot formation.

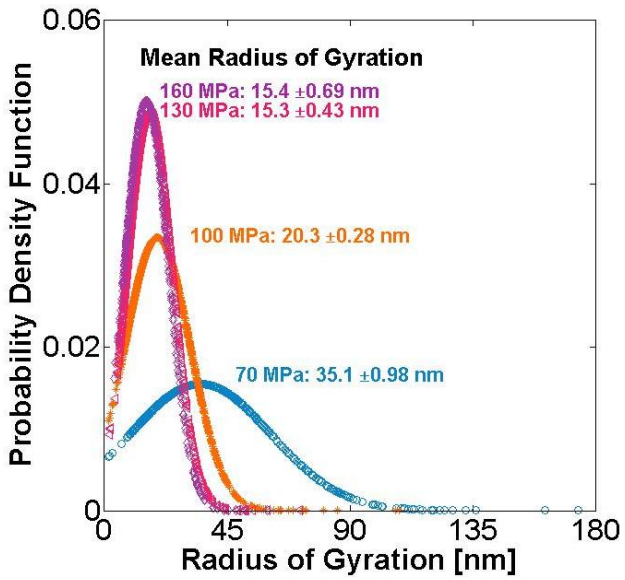

Figure 5. Probability density functions of radius of gyration of soot particles for various injection pressures. The mean radius of gyration and error range (estimated at 95% confidence for normal distribution) are noted for each injection pressure.

3. Up to a certain point, the number of particles increases with increasing injection pressure although both the projection area and radius of gyration decrease. This result implies that the agglomeration and growth of soot particle play a key role in determining the total number of soot particles.

Acknowledgments

Experiments were conducted at the Engine Research Laboratory in the School of Mechanical and Manufacturing Engineering at the University of New South Wales. Support for this research was provided by the Australian Research Council under the grant number DP110103762.

References

[1] Aizawa, T., Nishigai, H., Kondo, K., Yamaguchi, T., Nerva, J.G., Genzale, C., Kook, S. & Pickett, L.M., Transmission Electron Microscopy of Soot Particles Directly Sampled in Diesel Spray Flames - A Comparison between US#2 and Biodiesel Soot, *SAE Int. J. Fuels Lubr.*,**5(2)**, 2012, 665-673.

[2] Chandler, M.F., Tenh, Y. & Koylu, U.O., Diesel Engine Particulate Emissions: A Comparison of Mobility and Microscopy Size Measurements, *Proc. Combust.* Inst.,**31**, 2007, 2971-2979.

[3] Dodge, L., Simescu, S., Neely, G., Maymar, M., Dickey, D.W. & Savonen, C.L., Effect of Small Holes and High Injection Pressures on Diesel Engine Combustion, *SAE Tech. Paper*, 2002-01-0494, 2002.

[4] Dobbins, R.A. & Megaridis C.M., Morphology of Flame-Generated Soot as Determined by Thermophoretic Sampling, *Langmuir*,**3**, 1987, 254-259.

[5] Hu, B., Yang, B. & Koylu, U.O., Soot Measurements at the Axis of an Ethylene/Air Non-Premixed Turbulent Jet Flame, *Combust. Flame*,**134**, 2003, 93-106.

[6] Kook, S. & Pickett, L.M., Soot Volume Fraction and Morphology of Conventional and Surrogate Jet Fuel Sprays at 1000-K and 6.7-MPa Ambient Conditions, *Proc. Combust. Inst.*,**33**, 2011, 2911-2918.

[7] Kook, S. & Pickett, L.M., Soot Volume Fraction and Morphology of Conventional, Fischer-Tropsch, Coal-Derived, and Surrogate Fuel at Diesel Conditions, *SAE Int. J. Fuels Lubr.*,**5(2)**, 2012, 647-664.

[8] Pickett, L.M. & Siebers, D.L., Soot in Diesel Fuel Jets: Effects of Ambient Temperature, Ambient Density, and Injection Pressure, *Combust. Flame*,**138**, 2004, 114–135

[9] Lee, K.O., Cole, R., Sekar, R., Choi, M.Y., Kang, J.S., Bae, C.S. & Shin, H.D., Morphological Investigation of the Microstructure, Dimensions, and Fractal Geometry of Diesel Particulates, *Proc. Combust. Inst.*,**29**, 2002, 647-653.

[10] Neer, A. & Koylu, U.O., Effect of Operating Conditions on the Size, Morphology, and Concentration of Submicrometer Particulates Emitted from a Diesel Engine, *Combust. Flame*,**146**, 2006, 142-154.

[11] Vander Wal, R.L. & Choi, M.Y., Pulsed Laser Heating of Soot: Morphological Changes, *Carbon*,**37(2)**, 1999, 231-239.

[12] Zhu, J., Lee, K.O., Yozgatligil, A. & Choi, M.Y., Effects of Engine Operating Conditions on Morphology, Microstructure, and Fractal Geometry of Light-Duty Diesel Engine Particulates, *Proc. Combust. Inst.*,**30**, 2005, 2781-2789.